Ocean Engineering 155 (2018) 1–9

Contents lists available at ScienceDirect

Ocean Engineering

journal homepage: www.elsevier.com/locate/oceaneng

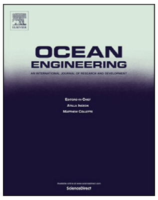

Inhibition of cloud cavitation on a flat hydrofoil through the placement of an obstacle

Lingxin Zhang[a,b], Ming Chen[a], Xueming Shao[a,*]

[a] *The State Key Laboratory of Fluid Power and Mechatronic Systems, Department of Mechanics, Zhejiang University, 310027 Hangzhou, China*
[b] *Key Laboratory of Soft Machines and Smart Devices of Zhejiang Province, 310027 Hangzhou, China*

ARTICLE INFO

Keywords:
Re-entrant jet
Cloud cavitation
Obstacle

ABSTRACT

Unsteady cavitation is an important topic due to its potential to cause huge damage to the hydraulic machinery. To control the shedding of cloud cavitation, the cavitation over a flat hydrofoil with an obstacle is investigated experimentally and numerically. A series of experiments around the flat hydrofoil without/with obstacle are carried out to study the evolution of cavitation. Periodic re-entrant jet and large shedding of cloud cavitation are observed in the case without obstacle, while the shedding of cloud cavitation in the case with obstacle is much weaker. Numerical simulations of the 2D unsteady cavitating flows around the hydrofoil are also performed. The transient and averaged fields of numerical simulations are presented and compared with the experimental data. The results show that in cases without obstacle, the averaged cavity length becomes longer with the decrease of the cavitation number. While in cases with obstacle, there is a range of cavitation number, in which the averaged cavity length almost keeps constant. The existence of obstacle changes the strength and direction of the transient re-entrant jet as well as the pressure distribution at the tail part of the cavity, leading to the weaker shedding of the cloud cavitation.

1. Introduction

Cavitation has received much attention since Rayleigh (1917) first introduced the issue of cavitation erosion on ship propeller. Various cavitation patterns could be observed on the surface of almost any type of hydrofoil as the cavitation number decreases: sheet/partial cavitation, cloud cavitation and super cavitation (Franc and Michel, 2004; Brennen, 2013). Partial cavitation is inherently unsteady in nature and causes oscillations of cavity length (Konno et al., 2002; Ida, 2004). The destabilization process results in the shedding of large bubbly vapor structure, called cloud cavitation. The collapse of cloud cavitation could generate huge pressure impact and cause damage on the nearby surface. Numerous observations and investigations of unsteady cavitation have been performed for flows around hydrofoils (Lush and Peters, 1982; Larrarte et al., 1995; Callenaere et al., 2001; Stanley et al., 2014) and internal flows such as in orifices and venturis (Stanley et al., 2011; De-Giorgi et al., 2013; Abdulaziz, 2014).

Furness and Hutton (1975) early mentioned that re-entrant jet is the main mechanism of cavitation instability. The dynamic behaviors of the cavitation in a venturi type nozzle were studied experimentally. Since then, considerable progresses have been made to prove re-entrant jet is the main reason of onset of cloud cavitation (Lush and Skipp, 1986; Le et al., 1993; Kawanami et al., 1997; Sato et al., 2013). On the other hand, other mechanisms of cavitation instability were also proposed. Kubota et al. (1992) considered that a shear layer separated at the cavity leading edge causes a jet into the cavity surface and then cloud cavitation is generated. Recently, Ganesh et al. (2016) introduced another mechanism of shock wave accounting for the shedding of the cloud cavitation. These new explanations remind us that the destabilization process of partial cavitation is very complicated, and besides the mechanism of re-entrant jet, other instability mechanisms may be dominant under certain conditions.

Many researchers were devoted to study the reason of the generation of re-entrant jet. Two kinds of explanations were proposed. One is, the collapse of the shedding cloud cavitation generates high pressure near the body. The transient pressure difference results in the formation of jet and cavitation instability (Leroux et al., 2004, 2005). However, other experiments show that the correlation between pressure pulses generated by the cloud collapse and the re-entrant jet motion is not obvious (Coutier-Delgosha et al., 2003). Another explanation is, the adverse pressure gradient at the end of cavity is the main reason of motion of the re-entrant jet (Callenaere et al., 2001; Laberteaux and Ceccio, 2001). If

---

* Corresponding author.
E-mail address: mecsxm@zju.edu.cn (X. Shao).

https://doi.org/10.1016/j.oceaneng.2018.01.068
Received 11 July 2017; Received in revised form 4 December 2017; Accepted 15 January 2018

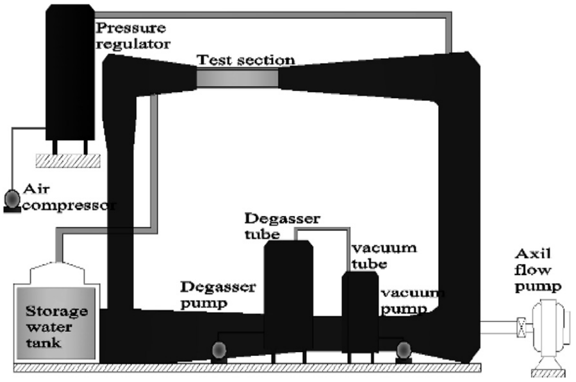

Fig. 1. Schematic of the cavitation tunnel.

the adverse pressure gradient decreases, the shedding of cloud cavitation would be reduced significantly. The thickness of the jet, which is directly related to the adverse pressure gradient, plays an important role in the instability of the cavitation. In a case of relatively thin cavity, a periodic re-entrant jet would be also observed. However, a strong interaction exists between the cavity interface and the re-entrant jet all along its upstream movement. Small vapor structure would be formed at the wake of the thin cavity (Stanley et al., 2014). Callenaere et al. (2001) thought that large shedding of cloud cavitation would happen when the ratio of the re-entrant jet thickness to the cavity thickness ranges from 15% to 35%.

Several works have paid attention on the inhibition of cavitation and its instability. A pioneer work of geometry optimization of hydrofoils was carried out by Eppler (1980). Their results show that cavitation on hydrofoil can be delayed and reduced due to changing the hydrofoil section. Yamaguchi et al. (1986) introduced this approach to inhibit the cavitation on propeller. Since then, a group of researchers made efforts to improve the related works (Dang, 1998; Zeng and Kuiper, 2009). To control the stability of cavitation, the approach of air injection was also considered (Arndt et al., 1995; Akbarzadeh and Akbarzadeh, 2016). Considering the phenomenon of periodic re-entrant jet, Kawanami et al. (1997) placed an obstacle on a NACA-type hydrofoil to obstruct the re-entrant jet, thus to reduce the shedding of cloud cavity. As the results show, the shedding of cloud cavitation reduces obviously under their experiment condition. However, few experiments or simulations have been performed to study the relationship between the obstacle and the re-entrant jet.

In present work, the cavitation over a flat hydrofoil without/with an obstacle is investigated experimentally and numerically, respectively. The placement of the obstacle is used to inhibit the shedding of cloud cavitation. The focus of experiments is on the observations of the cavitation under different conditions. 2D numerical simulations are performed to predict the fields of the unsteady cavitating flows. The features of the re-entrant jet in cases with/without the obstacle are presented. In addition, the correlation between the cavitation behavior and the adverse pressure gradient is discussed.

2. Method

2.1. Experiment condition

All the measurements and visualizations are carried out in the cavitation tunnel of Zhejiang University. The tunnel, as shown in Fig. 1, is an upright close-loop structure with height of 5.8 m and width of 5.2 m. The test section is about 1000 mm long and has a rectangular area of 200 × 200 mm. The tunnel has the basic functions of pressurization, depressurization and degassing. For the process of degassing, the vacuum pump offers low pressure to eliminate the gas in the water. The design water speed is 0–12 m/s, and minimal pressure is 0.1atm. All the experiment parameters, such as pressure, water speed, and cavitation number are controlled by operating an electronic touch screen. The angle of attack is adjusted by a control device which has an accuracy of 0.1°.

The sizes of the used flat hydrofoil, as shown in Fig. 2, are 150 × 200 × 12 mm, in which the chord length $c = 150$ mm. The hydrofoil is fixed at zero angle of attack. Experiments are performed first for a flat hydrofoil without obstacle, then for a flat hydrofoil with a full-span obstacle, which is 2 mm high and 2 mm wide. The obstacle is placed at the location of $0.37c$ from the leading edge. The images of cavitation are recorded by a Photron SA4 high-speed camera with the frame rate of 5000 fps and the resolution of 1024 × 800 pixels.

In the experiments, the environment pressure in the tunnel would be reduced to a level around 0.3atm, and then the flow speed will be controlled by the axial pump. The cavitation number is defined as:

$$\sigma = \frac{p_\infty - p_v}{\frac{1}{2}\rho U_0^2}, \tag{1}$$

where p_∞ is the environment pressure, p_v is the liquid saturation pressure, ρ is the density of water, and U_0 is the flow speed.

2.2. Numerical method

Most numerical models of cavitating flow assume that the fluids are homogeneous and isothermal, and employ either an appropriate equation of state (Coutier-Delgosha et al., 2003; Liu et al., 2004) or a transport equation (Merkle et al., 1998; Kunz et al., 2000; Morgut et al., 2011; Chen et al., 2015) to calculate the density of the mixture. In an Equation of State (EOS) model, a density-pressure dependency is needed to solve the rapid phase change process between two phases. Numerical methods for EOS models always refer to the density-based algorithm which is commonly employed in aerodynamics computations (Song and He, 1998). Transfer Equation Model (TEM) employs a phase transfer equation which reflects the mass conservation law. Typically, a pressure-based algorithm is used for the computation of cavitating flows with TEMs (Kunz et al., 2000; Senocak and Shyy, 2002; Zhang and Khoo, 2013). Here, we present our pressure-based numerical method by using Schnerr-Sauer cavitation model (Schnerr and Sauer, 2001) simply.

The governing equations of unsteady turbulent cavitating flows are given by:

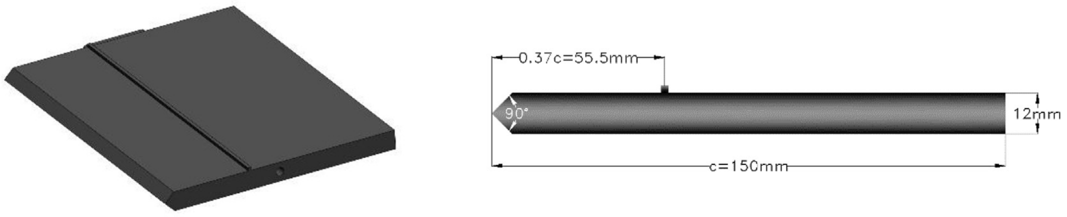

(a)

(b)

Fig. 2. Model of flat hydrofoil with obstacle: (a)3D view, (b) Side view.